Electromagnetic Wave Propagation in Media with Indefinite Permittivity and Permeability Tensors

D. R. Smith and D. Schurig

Physics Department, University of California–San Diego, La Jolla, California 92093

(Received 25 June 2002; published 21 February 2003)

We study the behavior of wave propagation in materials for which not all of the principal elements of the permeability and permittivity tensors have the same sign. We find that a wide variety of effects can be realized in such media, including negative refraction, near-field focusing, and high impedance surface reflection. In particular, a bilayer of these materials can transfer a field distribution from one side to the other, including near fields, without requiring internal exponentially growing waves.

DOI: 10.1103/PhysRevLett.90.077405 PACS numbers: 78.20.Ci, 42.25.–p, 78.67.–n, 84.40.–x

The range of available electromagnetic material properties has been broadened by recent developments in structured media, notably photonic band gap materials and metamaterials. These media have allowed the realization of solutions to Maxwell's equations not available in naturally occurring materials, fueling the discovery of new physical phenomena and the development of devices.

Photonic crystal effects typically occur when the wavelength is on the same order or smaller than the lattice constant of the crystal. Metamaterials, on the other hand, have unit cell dimensions much smaller than the wavelength of interest. A homogenization process, not unlike that applied in Ref. [1], can allow the otherwise complicated composite medium to be described conveniently by a permittivity tensor ($\boldsymbol{\varepsilon}$) and a permeability tensor ($\boldsymbol{\mu}$), rather than by band diagrams.

In 2000, it was shown experimentally that a metamaterial composed of periodically positioned scattering elements, all conductors, could be interpreted as having simultaneously a negative effective ε and a negative effective μ [2]. A medium with simultaneously isotropic and negative ε and μ supports propagating solutions whose phase and group velocities are antiparallel; equivalently, such a material can be rigorously described as having a negative index of refraction [3,4]. An experimental observation of negative refraction was reported using a metamaterial composed of wires and split ring resonators deposited lithographically on circuit board material [5].

The prospect of negative refractive materials has generated considerable interest, as this simply stated material condition suggests the possibility of extraordinary wave propagation phenomena, including near-field focusing [6]. So remarkable have been the claims surrounding negative refraction, that some researchers have been prompted to examine critically the achievability of negative refraction in existing metamaterials [7,8]. While such concerns might appear relevant in the context of frequency-dispersive materials, the interpretation of these structured materials as negative refractive has been entirely consistent with all aspects of reported experimental data [2,5], as well as with numerical simulations of both monochromatic and modulated beams [9,10]. For the purposes of this Letter, we thus assume that the descriptions presented here will be applicable to real materials, although the extent to which this is true remains a topic of active pursuit [11].

Lindell *et al.* [12] have shown that the property of negative refraction is not confined to materials with negative definite $\boldsymbol{\epsilon}$ and μ tensors, but can be expected to occur in certain classes of uniaxially anisotropic media. We explore here the general electromagnetic solutions associated with these anisotropic media, focusing on combinations of such media that provide access to the underlying properties. While there is a substantial reflection coefficient for non-normal waves incident on an anisotropic material from an isotropic material (or free space), due to the difference in dispersion properties of the two materials, a highly transmissive composite structure composed of layers of positively and negatively refracting anisotropic materials can be formed. As a specific example, we present an analysis of a compensated bilayer that produces subwavelength near-field focusing, but mitigates the thickness and loss limitations of the isotropic "perfect lens."

To simplify the proceeding analysis, we assume a linear material with $\boldsymbol{\varepsilon}$ and $\boldsymbol{\mu}$ tensors that are simultaneously diagonalizable,

$$\boldsymbol{\varepsilon} = \begin{pmatrix} \varepsilon_x & 0 & 0 \\ 0 & \varepsilon_y & 0 \\ 0 & 0 & \varepsilon_z \end{pmatrix}, \qquad \boldsymbol{\mu} = \begin{pmatrix} \mu_x & 0 & 0 \\ 0 & \mu_y & 0 \\ 0 & 0 & \mu_z \end{pmatrix}. \quad (1)$$

Metamaterials can be readily constructed that closely approximate these $\boldsymbol{\varepsilon}$ and $\boldsymbol{\mu}$ tensors, with elements of either algebraic sign. In fact, the scattering elements comprising the metamaterials used to demonstrate negative refraction [5,13] are appropriate building blocks for the classes of materials to be discussed here (see Fig. 1).

We apply the term *indefinite* to anisotropic media in which not all of the principal components of the $\boldsymbol{\varepsilon}$ and $\boldsymbol{\mu}$

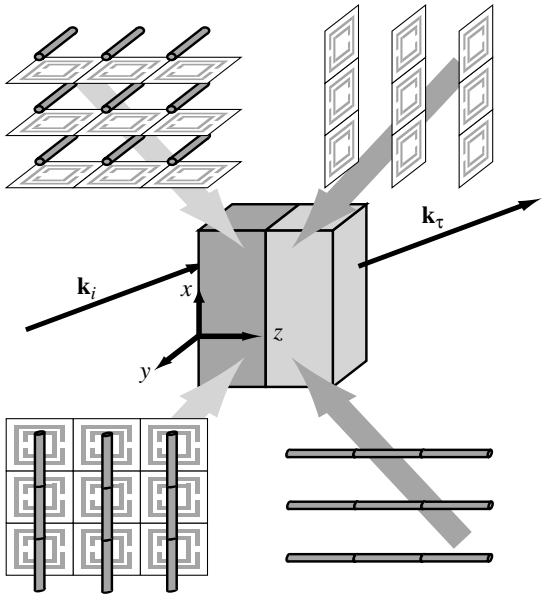

FIG. 1. A bilayer composed of indefinite media implemented using split ring resonators and straight wires. The structures in the top of the figure implement *never cutoff* media for electric y polarization. Top left is negative refracting and top right is positive refracting. The structures in the bottom of the figure do the same for magnetic y polarization.

tensors have the same sign. We will consider here layered media with surfaces normal to one of the principal axes, which we define to be the z axis. We assume in our analysis a plane wave with the electric field polarized along the y axis having the specific form

$$\mathbf{E} = \hat{\mathbf{y}} e^{i(k_x x + k_z z - \omega t)}, \tag{2}$$

though it is generally possible to construct media that are polarization independent, or that exhibit different classes of behavior for different polarizations. The plane wave solutions specified by Eq. 2 satisfy the dispersion relation

$$k_z^2 = \varepsilon_y \mu_x \frac{\omega^2}{c^2} - \frac{\mu_x}{\mu_z} k_x^2. \tag{3}$$

Since we have no x or y oriented boundaries or interfaces, real exponential solutions, which result in field divergence when unbounded, are not allowed in those directions. Furthermore, k_x is restricted to be real. Also, since k_x represents a variation transverse to the surfaces of our layered media, it is conserved across the layers, and naturally parametrizes the solutions.

In the absence of losses, the sign of k_z^2 can be used to distinguish the nature of the plane wave solutions. $k_z^2 > 0$ corresponds to real valued k_z and propagating solutions. $k_z^2 < 0$ corresponds to imaginary k_z and exponentially growing or decaying (evanescent) solutions. When $\varepsilon_y \mu_z > 0$, there will be a value of k_x for which $k_z^2 = 0$. This value, which we denote k_c, is the cutoff wave vector separating propagating from evanescent solutions. From Eq. (3), this value is $k_c = \frac{\omega}{c}\sqrt{\varepsilon_y \mu_z}$. We identify four classes of media based on their cutoff properties:

	Media conditions		Propagation
Cutoff	$\varepsilon_y \mu_x > 0$	$\mu_x/\mu_z > 0$	$k_x < k_c$
Anti-cutoff	$\varepsilon_y \mu_x < 0$	$\mu_x/\mu_z < 0$	$k_x > k_c$
Never cutoff	$\varepsilon_y \mu_x > 0$	$\mu_x/\mu_z < 0$	All real k_x
Always cutoff	$\varepsilon_y \mu_x < 0$	$\mu_x/\mu_z > 0$	No real k_x

Note the analysis presented here is carried out at constant frequency, and that the term *cutoff* always refers to the transverse component of the wave vector, k_x, not the frequency, ω. Isofrequency contours, $\omega(\mathbf{k}) = \text{const}$, show the required relationship between k_x and k_z for plane wave solutions (Fig. 2).

The general relationship between the directions of energy and phase velocity for waves propagating within an indefinite medium can be found by calculating the group velocity, $\mathbf{v}_g \equiv \nabla_{\mathbf{k}} \omega(\mathbf{k})$. $\mathbf{v}_g$ specifies the direction of energy flow for the plane wave, and is not necessarily parallel to the wave vector. $\nabla_{\mathbf{k}} \omega(\mathbf{k})$ must lie normal to the isofrequency contour, $\omega(\mathbf{k}) = \text{const}$, as illustrated in Fig. 2. Calculation of $\nabla_{\mathbf{k}} \omega(\mathbf{k})$ from the dispersion relation, Eq. (3), determines which of the two possible normal directions yields increasing ω and is thus the correct group velocity direction. Performing an implicit differentiation of Eq. (3) leads to a result for the gradient that does not require square root branch selection, removing any sign confusion. To obtain physically meaningful results, a causal, dispersive response function, $\xi(\omega)$, must be used to represent the negative components of ε and μ, since these components are necessarily dispersive [14]. The response function should assume the desired (negative) value at the operating frequency, and satisfy the causality requirement that $\partial(\xi\omega)/\partial\omega \geq 1$ [4,14]. Combining this with the derivative of Eq. (3) determines which of the two possible normal directions applies, without specifying a specific functional form for the response function. Figure 2 relates the direction of the group velocity to a given material property tensor sign structure.

Having calculated the energy flow direction, we can determine the refraction behavior of indefinite media by applying two rules: (i) The transverse component of the wave vector, k_x, is conserved across the interface, and (ii) energy carried into the interface from free space must be carried away from the interface inside the media; i.e., the normal component of the group velocity, v_{gz}, must have the same sign on both sides of the interface. Figure 2 shows typical refraction diagrams for the three types of media that support propagation.

To illustrate the unique possibilities associated with indefinite media, we recall that a motivating factor in recent metamaterials research has been the propect of near-field focusing. A planar slab with isotropic $\varepsilon = \mu = -1$ can act as a lens with resolution well beyond the

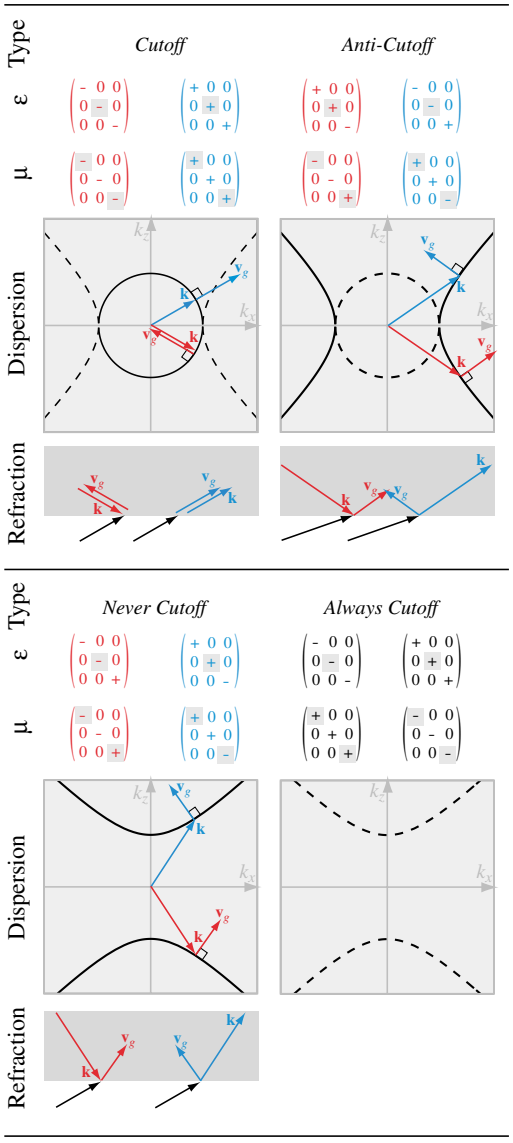

FIG. 2 (color). Material property tensor forms, dispersion plot, and refraction diagram for four classes of media. Each of these media has two subtypes: one positive (blue) and one negative (red) refracting, with the exception that *always cutoff* media do not support propagation and refraction. The dispersion plot shows the relationship between the components of the wave vector at fixed frequency. k_x (horizontal axis) is always real, k_z (vertical axis) can be real (solid line) or imaginary (dashed line). (The closed contours are shown circular, but can more generally be elliptical.) The same wave vector and group velocity vectors are shown in the dispersion plot and the refraction diagram. $\mathbf{v}_g$ shows direction only. The shaded diagonal tensor elements are responsible for the shown behavior for electric y polarization, the unshaded diagonal elements for magnetic y polarization.

diffraction limit [6]. It is difficult, however, to realize significant subwavelength resolution with an isotropic negative index material, as the required exponential growth of the large k_x field components across the negative index lens leads to extremely large field ratios. Sensitivity to material loss and other factors can significantly limit the subwavelength resolution.

By combining positive and negative refracting layers of *never cutoff* indefinite media, we can produce a compensated bilayer that accomplishes near-field focusing in a similar manner to the perfect lens, but with significant advantages. Figure 2 indicates that, for the same incident plane wave, the z component of the transmitted wave vector is of opposite sign for these two materials. Combining appropriate lengths of these materials results in a composite indefinite medium with unit transfer function. We can see this quantitatively by computing the general expression for the transfer function of a bilayer using standard boundary matching techniques [15],

$$\begin{aligned} T = 8[&e^{i(\phi+\psi)}(1-Z_0)(1+Z_1)(1-Z_2) \\ &+ e^{i(\phi-\psi)}(1-Z_0)(1-Z_1)(1+Z_2) \\ &+ e^{i(-\phi+\psi)}(1+Z_0)(1-Z_1)(1-Z_2) \\ &+ e^{i(-\phi-\psi)}(1+Z_0)(1+Z_1)(1+Z_2)]^{-1}. \end{aligned} \quad (4)$$

The relative effective impedances are defined as

$$Z_0 = \frac{q_{z1}}{\mu_{x1} k_z}, \qquad Z_1 = \frac{\mu_{x1}}{\mu_{x2}} \frac{q_{z2}}{q_{z1}}, \qquad Z_2 = \mu_{x2} \frac{k_z}{q_{z2}}, \quad (5)$$

where $\mathbf{k}$, $\mathbf{q}_1$, and $\mathbf{q}_2$ are the wave vectors in vacuum and the first and second layers of the bilayer, respectively. The individual layer phase advance angles are defined as $\phi \equiv q_{z1} L_1$ and $\psi \equiv q_{z2} L_2$, where L_1 is the thickness of the first layer and L_2 is the thickness of the second layer. If the signs of q_{z1} and q_{z2} are opposite as mentioned above, the phase advances across the two layers can be made equal and opposite, $\phi + \psi = 0$. If we further require that the two layers are impedance matched to each other, $Z_1 = 1$, then Eq. (4) reduces to $T = 1$ (the transfer function of free space is $T = e^{ik_z(L_1+L_2)}$). In the absence of loss, the material properties can be chosen so that this occurs for all values of the transverse wave vector, k_x. Transfer functions with varying amounts of loss added are shown in Fig. 3.

A proposed implementation is shown in Fig. 1. The elements shown in the top and bottom of the figure will implement media that focuses electric y-polarized and magnetic y-polarized waves, respectively. Combining the two structures forms a bilayer that is x-y isotropic due to the symmetry of the combined lattice. This symmetry and the property $\boldsymbol{\mu} = \boldsymbol{\varepsilon}$ yield polarization independence. The materials are formed from split ring resonators and wires with numerically and experimentally confirmed effective material properties [5]. Each split ring resonator orientation implements negative permeability along a single axis, as does each wire orientation for negative permittivity.

While compensated bilayers of indefinite media exhibit reduced impedance mismatch to free space and

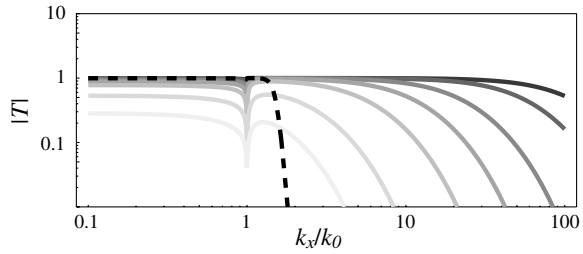

FIG. 3. Magnitude of the transfer function vs transverse wave vector, k_x, for a bilayer composed of positive and negative refracting *never cutoff* media. Material property elements are of unit magnitude and layers of equal thickness, λ. A loss producing imaginary part has been added to each diagonal component of $\boldsymbol{\varepsilon}$ and $\boldsymbol{\mu}$, with values 0.001, 0.002, 0.005, 0.01, 0.02, 0.05, and 0.1 for the darkest to the lightest curve. For comparison, a single layer, isotropic near field lens is shown dashed. The single layer has thickness λ, and $\varepsilon = \mu = -1 + 0.001i$.

high transmission, uncompensated semi-infinite indefinite media exhibit unique high reflection properties. Aside from *cutoff* materials, other classes of indefinite media have a reflection coefficient amplitude near unity for incident propagating waves. The phase of the reflection coefficient, however, varies, as illustrated here for positive refracting *anti-cutoff* media. The reflection coefficient for electric y polarization is given by

$$\rho = \frac{\mu_x k_z - q_z}{\mu_x k_z + q_z}, \tag{6}$$

where $\mathbf{k}$ and $\mathbf{q}$ are the wave vectors in vacuum and the media, respectively. For unit magnitude *anti-cutoff* material we have, from Eq. (3),

$$q_z^2 = -\frac{\omega^2}{c^2} + k_x^2 = -k_z^2. \tag{7}$$

Thus, $q_z = \pm ik_z$. The correct sign for positive refracting media, +, is determined by the requirement that the fields must not diverge in the domain of the solution. We then have

$$\rho = \frac{1 - i}{1 + i} = -i. \tag{8}$$

The magnitude of the reflection coefficient is unity, with a phase of $-90°$ for propagating modes of *all incident angles*. An electric dipole antenna placed $\lambda/8$ away from the surface would thus be enhanced by interaction with this "mirror" surface. Customized reflecting surfaces are of practical interest, as they enhance the efficiency of nearby antennas, while at the same time providing shielding [16,17]. Furthermore, an interface between unit *cutoff* and *anti-cutoff media* has no solutions that are simultaneously evanescent on both sides, i.e., surface modes (Fig. 2). In many communications applications, the energy lost to the excitation of surface modes is undesirable, as it represents loss of signal power.

In conclusion, we have begun to explore the properties of media with indefinite $\boldsymbol{\varepsilon}$ and $\boldsymbol{\mu}$ tensors. Consideration of layered structures has led to useful and interesting reflection and refraction behavior, including a new mechanism for subdiffraction focusing. We note that neither the analysis nor the fabrication of these media is complicated, and thus anticipate other researchers will quickly assimilate the principles and design structures with unique and technologically relevant properties.

We thank Claudio Parazzoli (Phantom Works, Boeing) for motivating this work. This work was supported by DARPA (Contract No. 972-01-2-0016), ONR (Contract No. N00014-00-1-0632), and AFOSR (Contract No. F49620-01-1-0440).

Note added.—While preparing this manuscript, we learned that a focal spot of $\lambda/25$ was experimentally achieved in a lumped circuit analog of the bilayer geometry [18].

[1] P. Halevi, A. A. Krokhin, and J. Arriaga, Phys. Rev. Lett. **82**, 719 (1999).
[2] D. R. Smith *et al.*, Phys. Rev. Lett. **84**, 4184 (2000).
[3] V. G. Veselago, Sov. Phys. Usp. **10**, 509 (1968).
[4] D. R. Smith and N. Kroll, Phys. Rev. Lett. **85**, 3966 (2000).
[5] R. A. Shelby, D. R. Smith, and S. Schultz, Science **292**, 79 (2001).
[6] J. B. Pendry, Phys. Rev. Lett. **85**, 3966 (2000).
[7] P. M. Valanju, R. M. Walser, and A. P. Valanju, Phys. Rev. Lett. **88**, 187401 (2002).
[8] N. Garcia and M. Nieto-Vesperinas, Phys. Rev. Lett. **88**, 207403 (2002).
[9] J. A. Kong, B. Wu, and Y. Zhang, Appl. Phys. Lett. **80**, 2084 (2002).
[10] D. R. Smith, D. Schurig, and J. B. Pendry, Appl. Phys. Lett. **81**, 2713 (2002).
[11] R. Ruppin, Phys. Lett. A **299**, 309 (2002).
[12] I.V. Lindell, S. A. Tretyakov, K. I. Nikoskinen, and S. Ilvonen, Microw. Opt. Technol. Lett. **31**, 129 (2001).
[13] D. R. Smith, S. Schultz, P. Markos, and C. M. Soukoulis, Phys. Rev. B **65**, 195104 (2002).
[14] L. D. Landau, E. M. Lifshitz, and L. P. Pitaevskii, in *Electrodynamics of Continuous Media* (Pergamon, New York, 1984), Chap. X.
[15] A. Yariv, *Optical Waves in Crystals : Propagation and Control of Laser Radiation* (Wiley, New York, 1984).
[16] D. Sievenpiper *et al.*, IEEE Trans. Microwave Theory Tech. **47**, 2059 (1999).
[17] K.-P. Ma, Y. Qian, and T. Itoh, IEEE Trans. Microwave Theory Tech. **47**, 1509 (1999).
[18] K. G. Balmain, A. A. E. Luttgen, and P. C. Kremer, IEEE Antennas Wireless Propag. Lett. **1**, 146 (2002).